Drying characteristics, kinetics model and effective moisture diffusivity of vacuum far-infrared dried Rehmanniae

Liu Yunhong*, Li Xiaofang, Zhu Wenxue, Luo Lei, Duan Xu, Yin Yong

(*College of Food and Bioengineering, Henan University of Science and Technology, Luoyang 471023, China*)

Abstract: Vacuum far-infrared radiation (VFIR) drying has recently received many attentions because of its effective and successful applications in drying some agricultural products. The VFIR drying of Radix Rehmanniae was conducted and Weibull distribution function was applied to fit the drying kinetics in this study. The results showed that the increase of radiation heater temperature and the decrease of chamber pressure could reduce drying time obviously. Compared with single diffusion equation, Weibull distribution function had higher precision to fit the drying curves of VFIR drying of Rehmanniae. The effective moisture diffusivity (D_{eff}) increased with the increase of heater temperature and the decrease of pressure. Scanning electron telescope (SEM) analysis showed that more porous surface could be observed after VFIR drying, which is beneficial to enhance moisture diffusivity and drying rate as well.

Keywords: vacuum far-infrared radiation drying, moisture ratio, effective moisture diffusivity, Rehmanniae, Weibull distribution function

DOI: 10.3965/j.ijabe.20160905.2082

Citation: Liu Y H, Li X F, Zhu W X, Luo L, Duan X, Yin Y. Drying characteristics, kinetics model and effective moisture diffusivity of vacuum far-infrared dried Rehmanniae. Int J Agric & Biol Eng, 2016; 9(5): 208－217.

1 Introduction

Radix Rehmanniae, or Rehmanniae, has been widely used in China as a kind of famous and common Chinese traditional medicinal material since ancient times. It is still used by Chinese doctor in current days for curing fever, hematemesis, hematuria, constipation, rheumatism and so on[1]. Nowadays, Rehmanniae is even increasingly used in other parts of Asia such as Japan, Korea, Malaysia, Phillipine etc. Rehmanniae should be dried after harvesting to avoid perishing and to keep its effective components as much as possible.

Post-harvest decay is one of the major factors that limit the extension of shelf-life of agricultural products and considerable medicinal materials. Dehydration through removing moisture from medicinal materials is aimed at achieving long shelf life and retaining high effective component contents[2]. Direct solar drying has traditionally been used for getting dried Rehmanniae, but this method is weather dependent and time consuming, and moreover, the samples might suffer the problems from contamination of dust, sand particles and insects. The convective drying, another conventional method, has been widely and commercially used in producing dried Rehmanniae in China, yet it easily results in undesirable quality degradation as well as limited drying rate.

Received date: 2015-08-02 **Accepted date:** 2015-12-20

Biographies: Li Xiaofang, Master candidate, research interests: deep processing of agricultural products, Email: 2465074335@qq.com; **Zhu Wenxue,** PhD, Professor, research interests: agricultural product drying technology, Email: zwx@haust.edu.cn; **Luo Lei**, PhD, Associate Professor, research interests: deep processing of agricultural products, Email: 13623896431@139.com; **Duan Xu**, PhD, Professor, research interests: agricultural product drying technology, Email: duanxu_dx@163.com; **Yin Yong**, Professor, research interests: deep processing of agricultural products, Email: yinyong@haust.edu.cn.

***Corresponding author: Liu Yunhong,** PhD, Associate Professor, research interests: agricultural product processing technology. Mailing address: College of Food and Bioengineering, Henan University of Science and Technology, No.263, Kaiyuan Road, Luoyang 471023, Henan Province, China. Tel: +86-379-64282342, Email: lyunhong@126.com.

Far-infrared radiation (FIR) drying has been investigated as a potential method for the drying of numerous foodstuffs, such as potato[3], longan[4], banana[5], apple[6], and so on. When FIR technology is used to dry moist materials, FIR energy impinges on and penetrates into the materials and then is converted into thermal energy[7]. FIR drying presents some advantages compared with conventional drying: shorter drying time, higher energy efficiency and lower air flow through the sample product[8]. FIR drying has been proven to be very effective on drying products with high moisture content.

Since most medicinal materials are heat-sensitive in nature and easily degrade at the presence of oxygen, it is desirable to dry them at low oxygen content and low temperature to preserve product quality[9]. Because water can evaporate at lower temperature under vacuum condition, vacuum is usually applied to produce low pressure and low oxygen content with other heating methods. Several researchers have reported their experiments on vacuum far-infrared radiation (VFIR) drying of some products. Mongprannet et al.[10] examined the drying behavior of the leaf parts of welsh onion adopting VFIR drying method. The results showed that the radiation intensity levels influenced dramatically the quality indicators of the products. The authors also determined the energy consumption of VFIR drying of onion and built a mathematical model[11]. Bazyma et al.[12] investigated the dependence between FIR energy and the process duration, and built polynomial relationship for mass discharge changes versus time during VFIR drying of several agricultural products. Swasdisevi et al.[13] developed a mathematical model to predict the moisture content and temperature of a banana slice during VFIR drying. Yet the literature about VFIR drying of Rehmanniae is pretty scarce until now.

Weibull distribution function was originally developed by a Swedish scientist named Weibull in 1939. Weibull distribution function has been widely utilized to describe the behavior of systems or events that is variable to some degree in several industries including material, medicine, thermodynamics and so on. In recent years, Weibull distribution function was applied to drying kinetics simulation. Several researchers have applied Weibull distribution function to simulate hot air drying kinetics of turmeric, mango and Aloe vera, respectively, and all of simulated results achieved high fitting precision[14-16]. Yet the application of Weibull distribution function in VFIR drying has not been found in existed literature.

The objective of this research was to develop a mathematical model based on Weibull distribution function to predict moisture ratio changes in Rehmanniae slices at different FIR heater's temperatures and under different pressures undergoing VFIR drying. The effects of heater's temperature and pressures on VFIR drying characteristics and effective moisture diffusivity (D_{eff}) were also to be investigated.

2 Materials and methods

2.1 Material

Fresh ripe Rehmanniae samples were obtained from a local special production base of Chinese herbs in Henan province, China and were stored in a refrigerator at 2-4^{o}C. Prior to the experiment, Rehmanniae samples with similar size were cut into 6.0±0.1 mm thick slices with a food slicer (MC30, Helian Co., China) and the thickness of each slice was measured using a vernier caliper (GL150, Guanglu Co., China). The initial moisture content of fresh Rehmanniae slices was determined by vacuum drying at 70°C for 24 h[17]. The initial moisture content of fresh Rehmanniae was measured in the range of 3.05-3.52 g/g (dry base).

2.2 Experimental VFIR dryer

A schematic of the self-fabricated VFIR dryer used in this work is shown in Figure 1. The dryer consists of two parts of lower chamber and upper chamber. The lower chamber contains a vacuum system including a vacuum pump (2XZ-4, Wanjing Co., China), a drying pot and an electromagnetic valve (DDC-JQ-A, Disai Co., China). The upper chamber mainly consists of a stainless steel drying chamber with inner dimensions of 45 cm × 45 cm × 45 cm. The pressure in the drying chamber can be adjusted by the vacuum system. An FIR heater made up of four 12 cm × 12 cm radiation

boards is installed at the top of the drying chamber. A weight sensor (precision 0.1 g, KS-516, Jingjiu Co., China) which links a weight indicator (XK-3190-A12, Yaohua Co., China), is set on the top of the chamber, and the other side of the sensor is connected to a tray holder. The mass change of samples is detected continuously and shown on the screen of the indicator. A stainless steel material tray, which has dimensions of 38 cm × 38 cm, can be put on the holder. Three Pt100 thermosensors (precision 0.1K, BD-WZP, Bodian Co., China) are installed in the chamber. One is put on the surface of the heater and is connected to a temperature controller which can display and adjust the temperature of the heater, and the temperature of the surface and the inside of materials can be measured by the other two sensors connected to a temperature display.

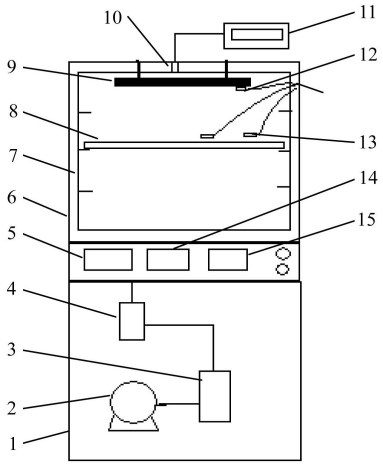

Note: 1. Lower chamber 2. Vacuum bump 3. Drying pot 4. Electromagnetic valve 5. Temperature display 6. Upper chamber 7. Tray holder 8. Material tray 9. Infrared radiation heater 10. Weight sensor 11. Weight indicator 12. Thermosensor for radiation board 13. Thermosensor for material 14. Pressure controller 15. Board temperature controller

Figure 1 Schematic of vacuum infrared radiation dryer

2.3 FIR heater

The FIR heater was manufactured by Henan University of Science and Technology. The ingredients constitution of the heater has been studied previously and optimized as 80% of ZrO_2, 15% of TiO_2, and 5% of other ingredients including MnO_2, Fe_2O_3, CuO, MgO and paraffin[18]. The FIR heater has strong infrared emittance in the wavelength range of 6-13 μm.

In order to verify the matching of the emissivity of FIR material and the absorbance of Rehmanniae, both of them were scanned by a Fourier transform infrared spectrometer (FTIR, Ventor70, Bruker Co., Germany). Some FIR materials were scraped and grounded with potassium bromide. A thin tablet was obtained by compressing with a pelleter, and then, was scanned with FTIR method. The spectrogram with wavenumber range of 400-4000 cm^{-1} was presented in Figure 2. Some fresh Rehmanniae were diced and pulped, and then were scanned with liquid-film method within wavenumber range of 400-4000 cm^{-1}, and the spectrogram was shown in Figure 3.

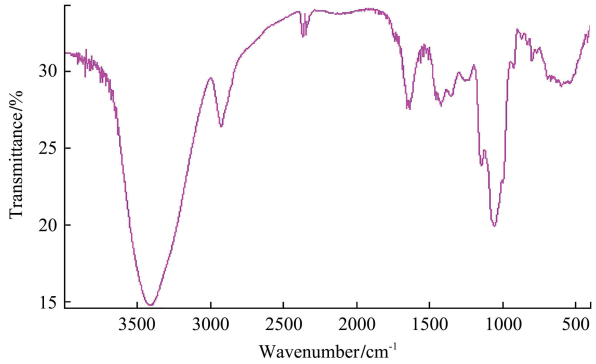

Figure 2 FTIR spectrogram of infrared radiation material

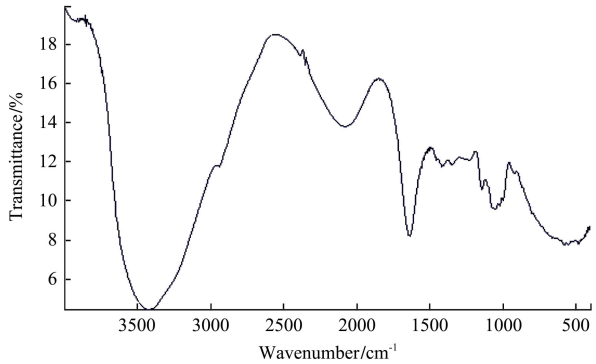

Figure 3 FTIR spectrogram of fresh Rehmanniae

According to Figure 2, there were several characteristic peaks for FIR material at the wavenumbers of 3412 cm^{-1}, 1637 cm^{-1}, 1057 cm^{-1} and 597 cm^{-1} with corresponding emissivity values of 82%, 56%, 72% and 54%, respectively. Pure water has strong absorbance peaks at the wavenumbers of 3425 cm^{-1}, 2100 cm^{-1}, 1634 cm^{-1} and 633 cm^{-1}, respectively. There are numerous ingredients in Rehmanniae, therefore small deviation was produced for characteristic peak area comparing with water, and the strong absorbance peaks existed at the wavenumbers of 3420 cm^{-1}, 2080 cm^{-1}, 1650 cm^{-1} and 600 cm^{-1}, respectively. Comparing Figure 2 with Figure 3, it can be concluded that high spectral matching could be achieved between the FIR material and Rehmanniae.

2.4 Experimental method

The dryer was run idle for about 30 min to achieve a desirable steady state in respect of pre-set experimental drying conditions before each drying experiment. About 200 g of sliced Rehmanniae were uniformly spread on the middle section of the tray with sample spread area of 24 cm×24 cm, and the distance between the tray and the FIR heater was fixed as 12 cm. The drying experiments were, therefore, conducted at heater temperatures of 353 K, 373 K, 393 K, 413 K and 433 K and under chamber pressures of 500 Pa, 1500 Pa, 5000 Pa, 15000 Pa and 50000 Pa, respectively. The mass values of the sample could be displayed on the indicator and were recorded every 30 min. The drying was ended when the continuous two records were the same.

Moisture content was calculated using the following equation[19]:

$$M = \frac{W - W_1}{W_1} \tag{1}$$

where, M is the moisture content, g water/g dry solid; W is the mass of sample at different times during drying, g; W_1 is dry matter of sample, g.

Because the equilibrium moisture content M_e was very low and could be negligible, the moisture ratio (MR) was simplified to M/M_0[20]:

$$MR = \frac{M - M_e}{M_0 - M_e} \approx \frac{M}{M_0} \tag{2}$$

where, M and M_0 are the moisture content at any given time and the initial moisture content, respectively, %.

2.5 Effective moisture diffusivity

Diffusivity is usually used to indicate the flow of moisture within materials during drying process. Assuming the main mechanism as being of diffusive nature, the experimental data for determination of diffusivity was interpreted by Fick's second diffusion equation:

$$\frac{\partial M}{\partial t} = D_{eff} \frac{\partial^2 M}{\partial x^2} \tag{3}$$

Rehmanniae slice is considered as an infinite slab because the thickness of the slice (6 mm) was much less than its diameter (about 40 mm). If the moisture movement by thermal gradient within the thin slab is considered as negligible, moisture transfer can be assumed to be a one-dimensional diffusion process in the upward direction from the bottom of the product toward the top surface. Other assumptions involved for diffusion analysis are as follows: (i) moisture is initially uniformly distributed throughout the sample, (ii) mass transfer is symmetric with respect to the centre and the shrinkage is negligible.

Therefore, the adequate initial and boundary conditions for slab in thickness L can be written as follows:

$t=0$, $0<x<L$, $M=M_0$

$t>0$, $x=L$, $M=M_e$

$t>0$, $x=0$, $\frac{dM}{dx}=0$

Thus, the analytical solution of Fick's equation is as follow[21]:

$$MR = \frac{8}{\pi^2} \sum_{n=0}^{\infty} \frac{1}{(2\pi+1)^2} \exp\left(-\frac{(2n+1)^2 \pi^2 D_{eff} t}{4L^2} \right) \tag{4}$$

For long drying times, MR<0.6, the equation can be simplified to the first term of the series with neglecting the higher order term.

$$MR = \frac{8}{\pi^2} \exp\left(-\pi^2 \frac{D_{eff} t}{4L^2} \right) \tag{5}$$

The effective moisture diffusivity D_{eff} could be calculated based on the equations above.

2.6 Microstructure analysis

The microstructure of dried Rehmanniae was observed by using a scanning electron telescope (SEM) (JSM-6010LA, Japan Electronics Co.). The magnification factor was set as 100 times. The porosity of dried Rehmanniae was analyzed by using Image-pro 6.0 software (Media Cybernetics Co., USA)[22].

2.7 Weibull distribution function

The Weibull distribution function used for fitting the drying kinetics of VFIR drying of Rehmanniae is shown as follow[14-16]:

$$MR = \exp\left[-\left(\frac{t}{\alpha} \right)^{\beta} \right] \tag{6}$$

where, α is scale parameter, min; β is shape parameter.

2.8 Statistical parameters

The coefficient of determination R^2, root mean square error RMSE and mean bias error MBE were chosen for

goodness of fit of model[23]:

$$R^2 = 1 - \frac{\sum_{i=1}^{N}\left(MR_{pre,i} - MR_{\exp,i}\right)^2}{\sum_{i=1}^{N}\left(MR_{pre,i} - MR_{\exp,i}\right)^2} \quad (7)$$

$$RMSE = \left[\frac{1}{N}\sum_{i=1}^{N}\left(MR_{pre,i} - MR_{\exp,i}\right)^2\right]^{1/2} \quad (8)$$

$$MBE = \frac{1}{N}\sum_{i=1}^{N}\left(MR_{pre,i} - MR_{\exp,i}\right) \quad (9)$$

where, the subscripts pre and exp represent predicted and experimental values, respectively.

2.9 Statistical analysis

All the statistical calculations and regression analyses were conducted by using SPSS system (version 10.0, USA).

3 Results and discussion

3.1 Drying curves

The effects of FIR heater's temperature on moisture ratio and surface temperature of Rehmanniae at the pressure level of 5000 Pa during VFIR drying are shown in Figure 4.

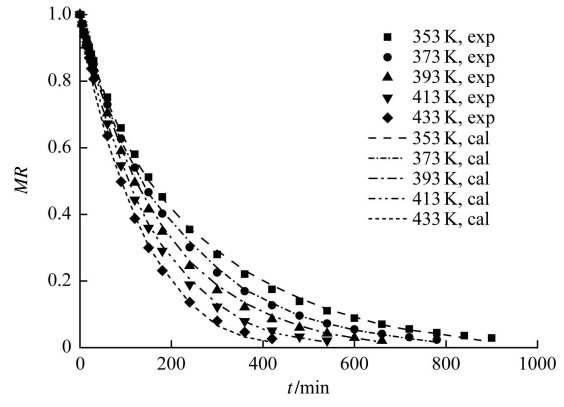

a. Drying curve

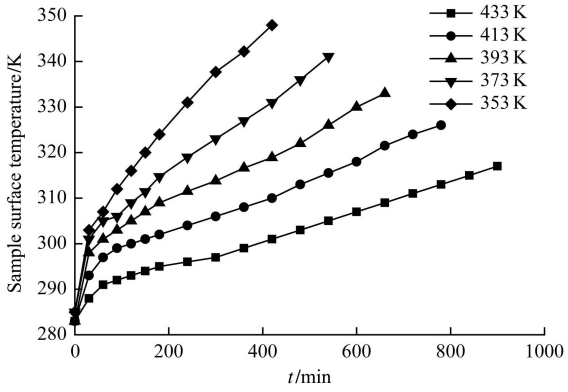

b. Sample surface temperature

Note: The exp and cal represent experimental and calculated data, respectively. The same below. The same below

Figure 4 Drying curves and temperature curves at different FIR heater's temperatures

Drying time reduced dramatically with the increase of FIR heater's temperature, and the drying times required were approximately 900 min, 780 min, 660 min, 540 min and 420 min at the heater's temperatures of 353 K, 373 K, 393 K, 413 K and 433 K, respectively. Moreover, both sample surface temperature rising rate and sample final temperature are higher with the increasing of FIR heater's temperature. According to Stefan-Boltzmann law[7], the increase of FIR heater's temperature results in the increase of radiation energy, and heat flux emitted to samples and the samples could absorb more heat quantities. Then the absorption of energy gives rise to a rapid temperature increase of the samples, resulting in the rising of water vapor pressure inside the sample, and subsequently, higher drying rate[24]. Moreover, FIR energy could penetrate into agricultural products with the depth of 1-4 mm[25], therefore the penetration of internal heating into the products could produce more uniform and better heating conditions compared with traditional contact heating[3].

The effects of chamber pressure on moisture ratio and sample surface temperature at FIR heater's temperature of 433K during VFIR drying are shown in Figure 5.

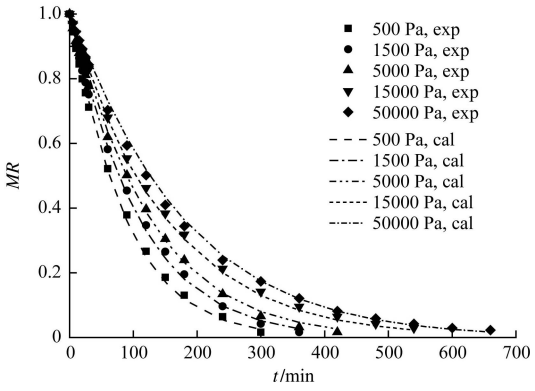

a. Drying curves

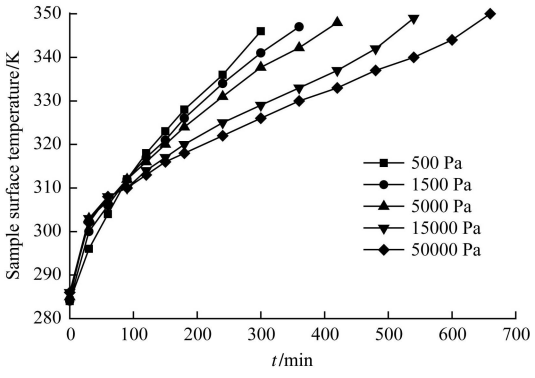

b. Sample surface temperature

Figure 5 Drying curves and temperature curves under different pressures

At fixed FIR heater's temperature, the drying time was shorter and the drying rate was higher with the decrease of chamber pressure. At the initial drying stage, the sample surface temperatures under lower pressures are lower than those under higher pressures. Yet as drying process goes on, higher sample surface temperature rising rates are achieved with the reduction of pressure, and the final sample surface temperatures are similar. With the decrease of pressure, water boils and evaporates at a lower temperature and escapes from the sample more easily[13]. Moreover, the water vapor pressure difference between samples and the chamber was enlarged with the reduction of pressure, resulting in higher evaporation speed of the water in samples. The effect of pressure on drying characteristics is as the same as the conclusion of Alibas[26], who reported that lower pressure could shorten drying time.

3.2 Development of drying mathematical model

Weibull distribution function was applied to fit the drying curves of the VFIR drying of Rehmanniae, and the results are listed in Table 1. The R^2, *MBE* and *RMSE* ranged at 0.9910-0.9996, −0.0081-0.0057 and 0.0032-0.0175, respectively. All the R^2 were close to 1, and all the values of *RMSE* and *MBE* were extremely small. So, it can be concluded that high fitting precision is achieved with Weibull distribution function.

Table 1 Fitting parameters, fitting precision indexes and moisture diffusive coefficient of Weibull distribution function and fitting precision indexes of single diffusion equation

parameter		Weibull distribution function				Single diffusion equation			
Heater temperature, *T*/K	Chamber pressure, *P*/Pa	α	β	R^2	*MBE*	*RMSE*	R^2	*MBE*	*RMSE*
353	500	162.3317	0.9178	0.9967	0.0048	0.0081	0.9616	0.0085	0.0788
373	500	143.3808	0.9570	0.9926	0.0031	0.0071	0.9655	0.0082	0.0234
393	500	128.2351	0.9980	0.9981	-0.0030	0.0084	0.9787	0.0063	0.0124
413	500	108.8232	1.0246	0.9973	0.0026	0.0074	0.9712	0.0045	0.0089
433	500	88.9234	1.0552	0.9988	-0.0036	0.0081	0.9723	0.0084	0.0104
353	1500	193.8869	0.9239	0.9982	-0.0048	0.0148	0.9731	-0.0071	0.0082
373	1500	171.3697	0.9624	0.9929	0.0031	0.0071	0.9838	-0.0036	0.0191
393	1500	154.9285	1.0025	0.9931	-0.0005	0.0057	0.9818	-0.0021	0.0378
413	1500	130.6378	1.0303	0.9948	0.0051	0.0081	0.9752	0.0049	0.0140
433	1500	106.8635	1.0644	0.9935	-0.0042	0.0068	0.9757	-0.0059	0.0091
353	5000	226.6564	0.9234	0.9991	0.0024	0.0064	0.9741	0.0052	0.0071
373	5000	196.9678	0.9617	0.9925	-0.0074	0.0175	0.9694	-0.0082	0.0159
393	5000	177.4437	1.0025	0.9947	0.0057	0.0092	0.9614	0.0123	0.0849
413	5000	149.8775	1.0287	0.9956	-0.0018	0.0050	0.9673	0.0101	0.0638
433	5000	122.1469	1.0643	0.9926	-0.0017	0.0032	0.9803	-0.0094	0.0434
353	15000	301.1714	0.8896	0.9962	0.0018	0.0043	0.9834	0.0053	0.0136
373	15000	256.4213	0.9153	0.9910	-0.0081	0.0091	0.9801	-0.0092	0.0152
393	15000	227.5610	0.9524	0.9937	-0.0074	0.0157	0.9841	-0.0081	0.0164
413	15000	191.3368	0.9809	0.9952	-0.0038	0.0084	0.9798	0.0042	0.0082
433	15000	154.8196	1.0175	0.9948	-0.0052	0.0101	0.9684	-0.0068	0.0162
353	50000	326.3289	0.8637	0.9944	-0.0027	0.0051	0.9724	-0.0049	0.0088
373	50000	283.3654	0.8996	0.9951	0.0039	0.0104	0.9782	0.0051	0.0123
393	50000	253.6656	0.9371	0.9996	0.0013	0.0038	0.9889	-0.0041	0.0085
413	50000	210.3575	0.9641	0.9921	0.0042	0.0071	0.9643	0.0072	0.0510
433	50000	171.2433	1.0022	0.9952	0.0032	0.0078	0.9652	0.0062	0.0398

To further verify the fitting suitability of Weibull distribution function for VFIR drying of Rehmanniae, single diffusion equation was selected as reference to fit the drying curves. The single diffusion equation is commonly used to fit drying curves of different drying processes and the equation is presented as following[27]:

$$MR=A\exp(-kt) \quad (10)$$

where, A and k are model parameters.

The fitting precision indexes of the single diffusion equation are also listed in Table 1. The value ranges of R^2, *MBE* and *RMSE* were 0.9614-0.9889, −0.0094-0.0123 and 0.0071-0.0849, respectively. Compared with the fitting precision indexes of the single diffusion equation, the R^2 values of Weibull distribution function were much higher, and the Values of *RMSE* and *MBE* were obviously smaller. Therefore the comparison result indicated that Weibull distribution function is more suitable to describe the drying kinetics of VFIR drying of Rehmanniae.

The values of the scale parameter α and shape parameter β are predicted in Table 1. The value of scale parameter equals approximately 63% of the total drying time needed and indicates the drying rate level of drying process. The α values decreased obviously with the increase of heater's temperature and the decrease of chamber's pressure, which meant the increase of radiation temperature as well as the decrease of pressure level could improve drying rate significantly. The shape parameter β is related with moisture diffusion mechanism during drying process. The β values increased with the increase of heater's temperature, which implied that moisture diffusion mechanism transforms from total internal moisture diffusion control to partial internal moisture diffusion control with increasing heater's temperature. The β values changed within a small range with the increase of chamber's pressure, which indicated that chamber pressure doesn't have significant effect on the internal moisture diffusion mechanism.

The equations of the scale parameter α and shape parameter β in Weibull distribution function could be expressed as follows through binary quadratic polynomial fitting:

$$\alpha = -315.881 + 1.1108T + 102.8262\ln P - 0.0006T^2 + 1.0627(\ln P)^2 - 0.237T\ln P \quad (R^2=0.9906) \tag{11}$$

$$\beta = -0.3832 + 0.0041T + 0.0662\ln P - 3.0571\times10^{-6}T^2 - 0.0047(\ln P)^2 \quad (R^2=0.9867) \tag{12}$$

3.3 Model verification

Weibull distribution function was used to simulate the drying kinetics of VFIR drying of Rehmanniae, and corresponding simulation results are presented in Figure 4 and Figure 5. As Figuers 4 and 5 showed, Weibull distribution function achieved a good fit to moisture ratio calculated from experimental data for VFIR drying of Rehmanniae. The values of R^2, *RMSE* and *MBE* were 0.9903, 0.011392 and −0.00435, respectively. In order to verify the prediction performance of the mathematical model, three additional experiments were conducted and the experimental data and model data are presented in Figure 6. Exp and Pre represented experimental and predicted data, respectively. The comparison showed that Weibull distribution function achieves quite good accuracy for the estimation of the moisture ratio during the drying process, at the heater's temperature and pressure of 363 K and 20 000 Pa, 383 K and 3000 Pa, 403 K and 1000 Pa, respectively. The corresponding values of R^2, RMSE and MBE equaled 0.9916, 0.009275 and 0.003317, respectively. Based on the simulation results, it could be concluded that Weibull distribution function achieves high precision for fitting the drying kinetics of VFIR drying of Rehmanniae and meets fitting requirement very well.

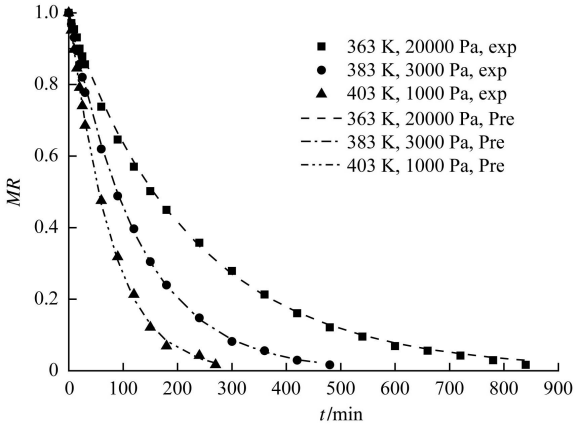

Figure 6 Comparison of experimental values and predicted values

3.4 Effective moisture diffusivity

The variations of effective moisture diffusivities during VFIR drying of Rehmanniae with different heater's temperatures and pressure levels are presented in Figure 7. It's obvious that the effective moisture diffusivity values increased with the increase of heater's temperature and the decrease of chamber pressure. Higher heater's temperature and lower pressure could increase the vapor pressure difference between the moisture inside material and the atmosphere outside material and then enhance moisture diffusion, resulting in

higher effective moisture diffusivity and shorter drying time. The analysis of variance (ANOVA) results about the effects of heater temperature and pressure level on D_{eff} values are listed in Table 2, and it could be concluded that both heater temperature and chamber pressure have extremely significant effects on effective moisture diffusivity.

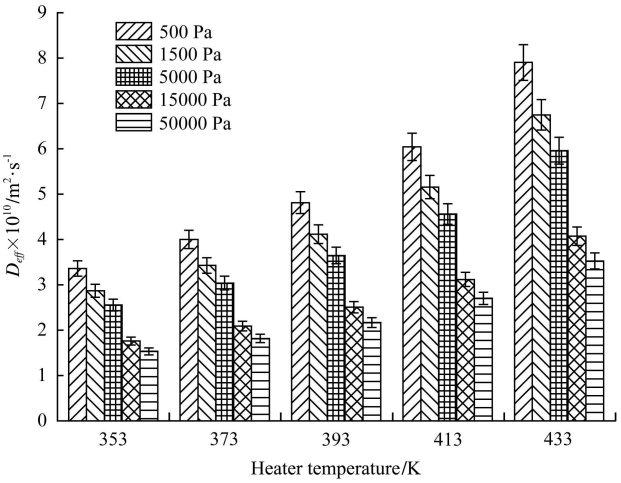

Figure 7 Effective moisture diffusivity of VFIR drying of Rehmanniae with different temperatures and pressure levels

Table 2 ANOVA for the effects of heater temperature and pressure level on $10^{10}\times D_{\text{eff}}$ values

Source	Sum of Squares	df	Mean square	*F* value	*p*-value
Pressure level	32.6802*	4	8.1701	45.6646	<0.001
Heater temperature	28.8297*	4	7.2074	40.2842	<0.001
Error	2.8626	16	0.1789	-	-
Total variation	64.3725	24			

Note: * Indicates extremely significant.

With the help of SEM, more information about the effect of VFIR drying treatment on microstructure and diffusivity of the samples could be found. The SEM pictures of Rehmanniae dried with traditional hot air drying and VFIR drying are presented in Figure 8. After hot air drying, Rehmanniae slices shrank obviously, therefore the microstructure of dried product was compact and few open pores appeared on the surface. Yet after VFIR drying, more, bigger and deeper open pores could be observed, which is beneficial to increase moisture diffusion inside the samples as well as drying rate. The porosity of Rehmanniae dried by VFIR method is 0.13±0.02, which is thirty percent higher than the value of Rehmanniae dried by hot air drying. Vacuum drying condition could enlarge the difference between the pressure inside samples and drying atmosphere, which reduces the shrinkage of samples during drying and protect moisture diffusion tunnels inside. In addition, FIR heating could provide thermal energy and heating penetration to samples with higher thermal efficiency and better heating effect comparing with hot air drying, and is also helpful to produce open pores. Therefore, the higher vapor pressure difference along with the stronger moisture diffusion and evaporation at VFIR drying could cause more porous surface than the dried product with hot air drying, and is beneficial to increase moisture diffusivity.

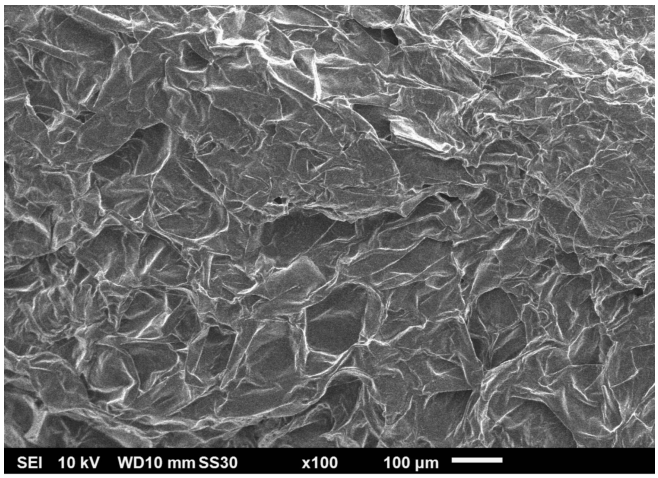

a. Hot air drying

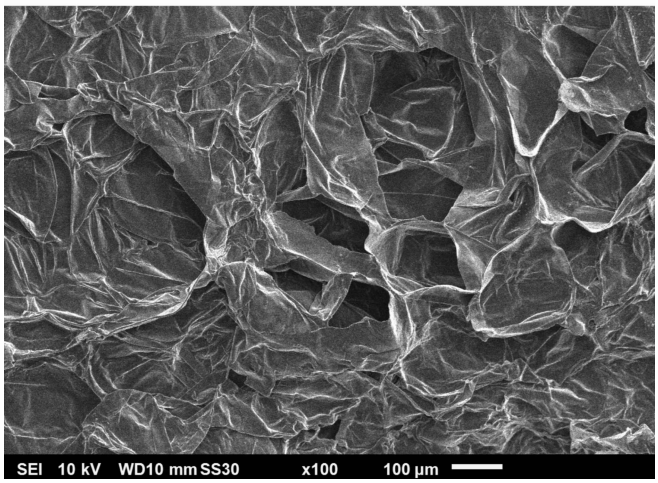

b. VFIR drying

Figure 8 SEM pictures of dried Rehmanniae with hot air drying and VFIR drying

4 Conclusions

The VFIR drying of Rehmanniae was conducted. Drying time reduced significantly with the increase of heater's temperature and the decrease of chamber's pressure, which indicated that both FIR heating and vacuum drying condition had the potential to improve

drying rate. A mathematical model based on Weibull distribution function was developed to simulate the moisture ratio of Rehmanniae undergoing VFIR drying, and the simulation results showed that Weibull distribution function could predict VFIR drying kinetics of Rehmanniae slices with quite good accuracy. The α values of the model indicated that the increase of radiation temperature as well as the decrease of pressure level could improve drying rate significantly. The β values imply that moisture diffusion mechanism transforms from total internal moisture diffusion control to partial internal moisture diffusion control with the increase of heater temperature, and the pressure in the chamber does not have a significant effect on the internal moisture diffusion mechanism during VFIR drying of Rehmanniae slices. The D_{eff} values increased with the increase of heater's temperature and decrease of pressure level, and both of them had significant effects on D_{eff} values. Based on SEM picture of dried product's microstructure, more porous surface could be observed after VFIR drying. Therefore, VFIR drying method is beneficial to increase drying rate and enhance moisture diffusivity. Future studies are crucial to elucidate the quality protection performance of VFIR drying method.

Acknowledgements

The authors express their sincere appreciation to the National Natural Science Foundation of China (Grant No. U1404334), the College Young Teachers Development Program of Henan province (Grant No. 2015GGJS-048) and the Science and Technology Project of Henan Province of China (Grant No. 12A210005 and 14B550005) for support this study financially.

[References]

[1] Liu Z, Lou Z, Ding X, Qi Y, Zhu Z, Chai Y. Global characterization of neutral saccharides in crude and processed Radix Rehmanniae by hydrophilic interaction liquid chromatography tandem electrospray ionization time-of-flight mass spectrometry. Food Chem., 2013; 141(3): 2633–2640.

[2] Liu Y H, Miao S, Wu J Y, Liu J X. Drying and quality characteristics of Flos Lonicerae in modified atmosphere with heat pump system. J. Food Process Eng., 2014; 37(1): 37–45.

[3] Afzal T M, Abe T. Diffusion in potato during far infrared radiation drying. J. Food Eng., 1998; 37(4): 353–365.

[4] Nathakaranakule A, Jaiboon P, Soponronnarit S. Far-infrared radiation assisted drying of longan fruit. J. Food Eng., 2010; 100(4): 662–668.

[5] Pekke M A, Pan Z, Atungulu G G, Smith G, Thompson J F. Drying characteristics and quality of bananas under infrared radiation heating. Int J Agric & Biol Eng, 2013; 6(3): 58–70.

[6] Timoumi S, Mihoubi D, Zagrouba F. Shrinkage, vitamin C degradation and aroma losses during infra-red drying of apple slices. LWT-Food Sci. Technol., 2007; 40(9): 1648–1654.

[7] Ginzburg A S. Application of Infrared Radiation in Food Processing. London: Chemical and Process Engineering Series. Leonard Hill, 1969.

[8] Ratti C, Mujumdar A S. Infrared drying. 2nd ed. In: Mujumdar, A.S. (Ed.), Handbook of Industrial Drying, vol. 1. New York: Marcel Dekker, 1995.

[9] Liu Y, Miao S, Wu J, Liu J, Yu H, Duan X. Drying characteristics and modelling of vacuum far-infrared radiation drying of Flos Lonicerae. J. Food Process. Pres., 2015; 39(4): 338–348.

[10] Mongpraneet S, Abe T, Tsurusaki T. Accelerated drying of welsh onion by far infrared radiation under vacuum conditions. J. Food Eng., 2002; 55(2): 147–156.

[11] Mongpraneet S, Abe T, Tsurusaki T. Kinematic model for a far infrared vacuum dryer. Dry. Technol., 2004; 22(7): 1675–1693.

[12] Bazyma L A, Guskov V P, Basteev A V, Lyashenko A M, Lyakhno V, Kutovoy V A. The investigation of low temperature vacuum drying processes of agricultural materials. J. Food Eng., 2006; 74(3): 410–415.

[13] Swasdisevi T, Devahastin S, Sa-Adchom P, Soponronnarit S. Mathematical modeling of combined far-infrared and vacuum drying banana slice. J. Food Eng., 2009; 92(1): 100–106.

[14] Blasco M, Garcia-Perez J V, Bon J, Carreres J E, Mulet A. Effect of blanching and air flow rate on turmeric drying. Food Sci. Technol. Int., 2006; 12(4): 315–323.

[15] Corzo O, Bracho N, Alvarez C. Weibull model for thin-layer drying of mango slices at different maturity stages. J. Food Process. Pres., 2010; 34(6): 993–1008.

[16] Miranda M, Vega-Galvez A, Garcia P, Scala K D, Shi J, Xue S, et al. Effect of temperature on structural properties of Aloe vera (Aloe barbadensis miller) gel and Weibull distribution for modeling drying process. Food Bioprod. Process., 2010; 88(2): 138–144.

[17] AOAC. Official method of analysis. Association of Official Analytical Chemists, Arlington, VA, 1990.

[18] Liu J X, Li H T, Zhu W X, Zhang Y X. Study on

Zirconium and Titanium far-infrared drying ceramic radiator. Transaction of the CSAM, 2006; 37(8): 221–223. (in Chinese with English abstract)

[19] Midilli A. Determination of pistachio drying behavior and conditions in a solar drying system. Int. J. Energ. Res., 2001; 25(8): 715–725.

[20] Togrul H. Simple modeling of infrared drying of fresh apple slices. J. Food Eng., 2005; 71(3): 311–323.

[21] Crank J. Mathematics of diffusion. 2nd ed. London: Oxford University Press, 1975.

[22] Wang J Z, Zheng X, Wan N, Lin G X, You Y. Fractal character of the pore structure of dehulled rapeseed cake based on scanning electron microscopy image analysis. Transaction of the CSAE, 2008; 24(3): 16–20. (in Chinese with English abstract)

[23] Midilli A, Kucuk H. Mathematical modeling of thin layer drying of pistachio by using solar energy. Energy Convers. Manage., 2003; 44: 1111–1122.

[24] Wu B, Pan Z, Qu W, Wang B, Wang J, Ma H. Effect of simultaneous infrared dry-blanching and dehydration on quality characteristics of carrot slices. LWT-Food Sci. Technol., 2014; 57(1): 90–98.

[25] Pan Y K, Wang X Z, Liu X D. Modern drying technology. Beijing: Chemical Industry Press, 2007.

[26] Alibas I. Microwave, vacuum, and air drying characteristics of collard leaves. Drying Technol., 2009; 27(11): 1266–1273.

[27] Luo D, Liu J, Liu Y, Ren G. Drying characteristics and mathematical model of ultrasound assisted hot-air drying of carrots. Int J Agric & Biol Eng, 2015; 8(4): 124–132.